14-day forecast of solar indices using interplanetary Lyman α background data

Eric Quémerais, Jean-Loup Bertaux

GEOPHYSICAL RESEARCH LETTERS, VOL. 29, NO. 2, 1018, 10.1029/2001GL013920, 2002

14-day forecast of solar indices using interplanetary Lyman α background data

Eric Quémerais and Jean-Loup Bertaux

Service d'Aéronomie du CNRS, Verrières le Buisson, France

Received 14 August 2001; revised 30 October 2001; accepted 12 November 2001; published 23 January 2002.

[1] We present a new method which can be used to forecast the variations of solar indices on the time scale of a half solar rotation. This method uses the Lyα interplanetary glow data obtained by the SWAN instrument on SOHO. We show how the maps of solar Lyα flux distributions derived from the SWAN data can be linked to the variation of activity on the solar disk. Active regions which are known to be brighter in Lyα radiation than the quiet sun illuminate more interplanetary H atoms through resonance scattering. This excess of illumination related to active regions is clearly seen in full-sky Lyα maps recorded by the SWAN instrument on SOHO. These maps include also those excesses resulting from active regions which are on the far side of the Sun, i.e. not visible to solar disk imagers near Earth. From these data, we can derive a farside to nearside flux ratio. This ratio is then used to predict the evolution of solar indices like the solar Lyα flux seen at Earth, the 10.7cm radio flux or the MgII solar index. This technique could be used in the future to improve the quality of space weather forecast, in particular to predict atmospheric heating and increased orbital drag of sensitive spacecraft. *INDEX TERMS:* 7549 Solar Physics, Astrophysics, and Astronomy: Ultraviolet emissions, 7537 Solar Physics, Astrophysics, and Astronomy: Solar and stellar variability, 7536 Solar Physics, Astrophysics, and Astronomy: Solar activity cycle (2162), 7594 Solar Physics, Astrophysics, and Astronomy: Instruments and techniques

1. Introduction

[2] The interstellar hydrogen atoms present in the interplanetary medium can backscatter the solar H Lyα photons, creating the bright interplanetary UV glow. The SWAN instrument, which is one of the twelve instruments on-board the SOHO spacecraft [*Bertaux et al.*, 1995], has been recording the variations of the interplanetary glow from early 1996 to present, thus covering the last solar cycle minimum and all the ascending phase up to the present maximum. The glow pattern variations observed are either caused by changes in the hydrogen distribution or by changes in the solar Lyα illuminating flux.

[3] Changes in the interplanetary hydrogen distribution are themselves caused by solar cycle variations of the solar ionization rates (photo-ionization by EUV photon flux and charge-exchange with solar wind protons). Changes in the Lyα illuminating flux are easily identified because they display the periodicity of the solar rotation. *Bertaux et al.* [2000] have shown that the synoptic full-sky observations of the H Lyα background made by the SWAN photometer can be used to map relative variations of the solar Lyα illuminating flux.

[4] One interest for this mapping arises from the fact that increases in the solar H Lyα brightness are related to activity on the solar disk. Active regions are known to be much brighter in UV light than the quiet sun [*Fontenla et al.*, 1988], thus increasing the total emission from the solar disk. Because SWAN covers the full-sky (4π steradian) emission from interplanetary hydrogen, it is then possible to observe backscattered photons which originated from the farside of the Sun and to reconstruct the flux distribution from both near and far sides of the Sun. This gives information on the activity on the farside of the sun which cannot be seen by conventional disk imagers.

[5] The SWAN farside imaging technique has been developed and is now operational. Nearside and Farside Lyα flux pattern images are routinely displayed on the SOHO web page.

[6] In this paper, we are using one year of data from SWAN (year 2000) to quantitatively relate the spatial variations of the solar Lyα flux observed by SWAN with the time-dependent variations of several solar indices widely used by the Space Weather community. The aim of this study is to build an algorithm which will allow us to predict temporal variations of solar indices observed at Earth, two weeks (ie. half a solar rotation) in advance. This might be particularly useful for a better prediction of the atmospheric drag that is affecting the orbit of sensitive spacecraft. Indeed, solar EUV radiation heats up the upper atmosphere which increases the orbital drag and speeds up the orbital decay.

2. Linear Correlation Studies

[7] Each SWAN observation of the full-sky interplanetary glow takes roughly one day [*Bertaux et al.*, 1995]. New observations are performed every two or three days. In 2000, 172 full-sky observations were performed. From each full-sky observation, made on day D, we can derive the solar Lyα flux emitted in every direction from the sun relative to the subspacecraft value. Figure 1 illustrates this by showing a top view of the observing geometry in the ecliptic plane. The Earth's (or SOHO's) orbit is shown by the dashed circle. The position of the observer is labelled "DAY 0". The position 180 degrees apart, which is centered in front of the farside, is labelled "DAY + 13.5". Indeed, because of the solar rotation, the region of the sun which is in the center of the farside will be in front of the spacecraft half a solar rotation later. Assuming that we can neglect intrinsic variations of the solar Lyα on a scale smaller than half a solar rotation then we can say that the flux emitted toward "DAY + 13.5" will be seen at the Earth 13.5 days later. This applies to all directions represented in the figure. The time delay for any direction can be computed using the fact that 360 degrees correspond to a solar rotation as seen from the Earth (27 days). However, the longer the time interval is the less accurate the prediction will be.

[8] In what follows, we will study the case of the ratio of the two fluxes emitted toward "DAY + 13.5" and "DAY 0", i.e. 180 degrees apart. The first one is noted $F(180°)$ because it corresponds to a spacecraft position 180 degree apart from its actual position in ecliptic longitude. The second one is noted $F(0)$. Although, SWAN cannot look directly toward the Sun, the $F(0)$ flux value is found by interpolation of data obtained close to the Sun. For each SWAN full-sky observation, we have computed the ratio $F(180°)/F(0)$. It corresponds to the relative variation of the fluxes derived from the SWAN data.

0094-8276/02/2001GL013920

[9] For this study, we have selected the measurements of the solar Lyα integrated line flux published by *Woods et al.* [2000]. The composite data set used here was mainly obtained from SOLSTICE/UARS measurements. We have also used the MgII line ratio measured by the SUSIM/UARS instrument. The other two indices are the 10.7 cm solar flux (F10.7) which is widely used by the Space Weather community and the corrected index called "E10.7" [*Tobiska et al.*, 2000] which relies on both Lyα and F10.7 in its derivation.

[10] For each solar index s_i, we have computed the following ratio. If D notes the date of a SWAN observation, $s_i(D)$ corresponds to the index value at the same date. $s_i(D + 13.5)$ is the index value observed 13.5 days later. We have then computed the ratio $s_i(D + 13.5)/s_i(D)$. If we note r_i the ratios, the mean value is $\langle r_i \rangle$ and the standard deviation is $\sigma_i = \sqrt{< r_i^2 > - < r_i >^2}$. The scaled ratio is then equal to $(r_i - \langle r_i \rangle)/\sigma_i$. We use a scaled ratio to be able to compare the adequacy of the correlations. Indeed each ratio displays a different annual variation. This is quantitatively estimated by the value of σ_i. The F10.7 has a large annual variation whereas the MgII index has a small one. The resulting normalized ratios display similar annual variations.

[11] Table 1 displays the quantitative results of the linear fits. The first two columns give the mean ratio and standard deviation of the ratio noted σ_{ri} in 2000. The 3rd column gives the residual of the linear fit χ_{ri}. The 4th column gives the ratio of the residual with the standard deviation. Since each index has a different range of annual variation which is measured by σ_{ri}, the residual of the fit χ_{ri} must be scaled to σ_{ri} for comparison. The 5th column shows the correlation coefficient obtained for each index.

[12] Both 4th and 5th columns demonstrate that the best fit is obtained when the SWAN flux ratio index is compared with the solar Lyα flux values. This is not a surprise. Yet, we must discuss why the fit is not perfect and which are the limiting factors.

[13] If the Lyα glow intensity is proportional to the solar illuminating flux, one expects that the two ratios, solar flux ratio and SWAN flux ratio are identical. Yet, the study of our data shows a slope of 1.13 between the SWAN data in abscisse and the solar flux data in ordinate. This means that the modulations of the SWAN data are 13% smaller than the actual modulations seen in the solar Lyα illuminating flux data.

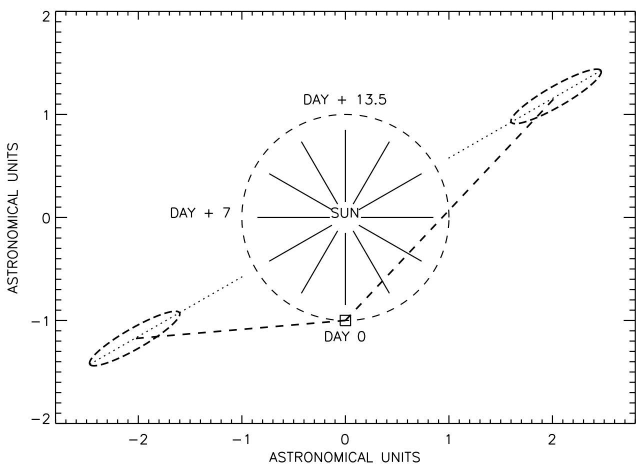

Figure 1. Sketch showing how the solar Lyα flux distribution can be retrieved in every direction. SWAN (position indicated by Day 0) sees the backscattered emission from every direction of space. The region where a large fraction of the photons are scattered (MER) is shown by the small ellipses. Its actual position depends on the density distribution of hydrogen but lies outside of the Earth orbit. Although there is a small parallax effect for values at 90 degrees, the spatial anisotropies of the illuminating flux can be retrieved with sufficient accuracy. We can study the ratio of the values emitted away from SOHO with the one emitted in the direction of SOHO. The value emitted in the direction opposite from SOHO corresponds to the surface of the sun which will be in the center of the visible disk half a solar rotation later (Day + 13.5).

Table 1. Study with Different Solar Indices

Index	Ratio	σ_{ri}	χ_{ri}	χ_{ri}/σ_{ri}	Correl
Lyα	1.010	0.097	0.044	0.459	0.885
F10.7	1.041	0.267	0.207	0.774	0.653
E10.7	1.030	0.213	0.152	0.715	0.689
MgII	1.001	0.017	0.008	0.474	0.872

[14] To understand this result, we must consider the fact that the total backscattered intensity is the sum of the two terms. The first one, which represents the largest fraction of the photons, corresponds to photons which are scattered only once between the sun and the observer. It is proportional to the number of photons emitted by the Sun. Because the inner heliosphere is optically thin, the backscattering area is spread over a rather large area (Figure 1). This could create a parallax effect as in the case of the observing geometries displayed in Figure 1. Luckily in the simple case of our study, there is no parallax effect because we consider only directions of sight at 0 and 180 degrees from the SOHO-Sun line (see Figure 1). For our study, the damping of the modulations cannot be explained by a parallax effect.

[15] The second term contributing to the intensity is due to photons which are scattered more than once. Although related to the solar illuminating flux, this term displays a damping of the solar modulations because photons may come from all areas of the Sun and be scattered many times before reaching the Sun. *Quémerais et al.* [1996] have computed the distribution function of the original direction of the observed photons. As the scattering order increases, the distribution function becomes less and less peaked thus damping any modulation of the solar illuminating flux.

[16] Some authors [*Scherer and Fahr*, 1996] have said that because the inner heliosphere is optically thin, the second term must be neglected. Other authors like *Hall* [1992], *Quémerais and Bertaux* [1993] and more recently *Quémerais* [2000] have estimated that the second term is not negligible in the inner heliosphere. They agree that the inner heliosphere is optically thin but argue that the medium becomes optically thicker with increasing solar distance and that the surrounding medium gives a significant contribution to the total intensity (See *Quémerais* [2000] for numerical estimates). We think that the fact that the SWAN flux ratio modulations are smaller (by 13%) than the actual modulations of the solar Lyα flux gives an observational proof that the optically thin approximation is not valid even inside the inner heliosphere.

3. Forecasting Algorithm

[17] The forecasting algorithm is built in the following manner. For any given solar index, we derive a relationship between the 13.5-day index value ratio, $s_i(D + 13.5)/si(D)$, and the SWAN farside to nearside flux ratio, $F(180°)/F(0)$ at day D. This empirical relationship is derived over a given period (one year here) preceding the observation date.

[18] For a given SWAN observation on day D, we derive the SWAN farside to nearside flux ratio. This ratio is then translated into an estimate of the 13.5-day index ratio using the relation previously determined. Figure 2 and Figure 3 show examples of this algorithm applied to all year 2000 SWAN observations in the case of the solar Lyα flux and of the F10.7 solar index. Once again, the quality of the fit is much better in the case of the solar Lyα flux.

[19] The estimate of 13.5-day index ratio at date D is then multiplied by the actual value of the index at day D. The result is an estimate of the index value at day D + 13.5, i.e. half a solar rotation later.

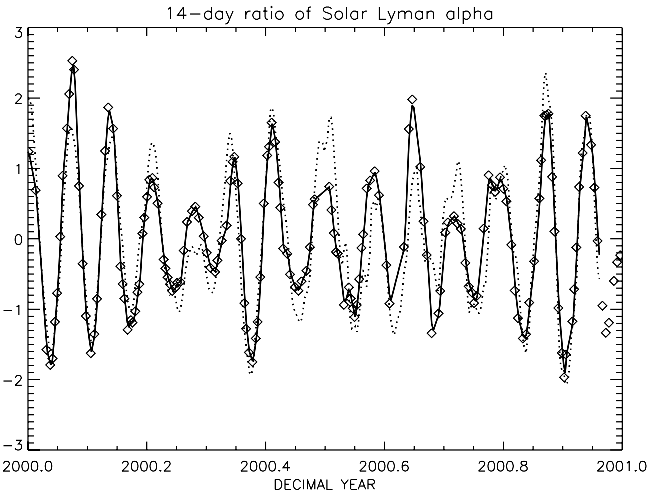

Figure 2. Comparison of the half solar rotation ratio of solar Lyα flux with the SWAN flux ratio index. The abscisse is the decimal year of the data. The dotted line shows the ratio of the Solar Lyα flux measured at $D + 13.5$ divided by the value at D. The thick line shows the predicted ratio using the correlation shown in the previous figure. Both curves are shown in units of normalized ratios as described in the text. The diamonds show the actual dates of SWAN observations. The result obained for the Solar Lyα flux is quite good. This shows that the total flux emitted by the sun does not change too much over half a solar rotation. The main cause for variation over this period of time is the solar rotation itself.

[20] In Table 2, we give for each of the solar index used here, the mean value in 2000 noted $\langle s_i \rangle$ and the standard deviation from the mean value in 2000 noted σ_i which measures the range of variation of the index in 2000. We have the relation, $\sigma_i = \sqrt{< s_i^2 > - < s_i >^2}$.

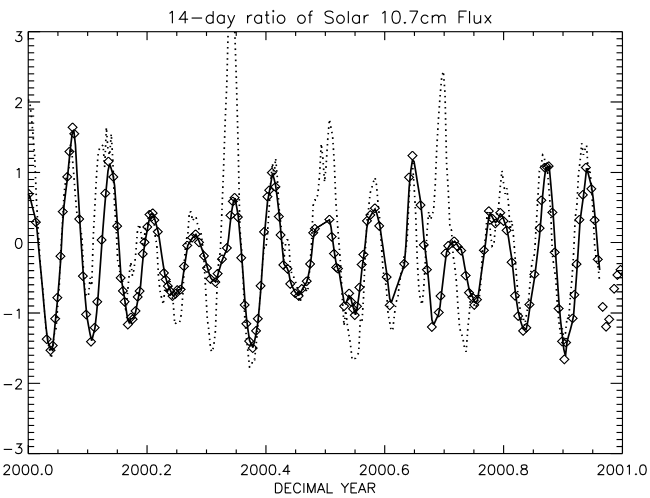

Figure 3. Comparison of the half solar rotation ratio of the 10.7cm solar flux with the SWAN flux ratio. The ordinate is in units of normalized ratio (Ratio value minus mean ratio and divided by standard deviation of ratio). As in the previous figure, the dotted line shows the ratio of the index values measured at date $D + 13.5$ and D. The thick line shows the predicted ratio using the correlation shown in Figure 2. The diamonds show the actual dates of SWAN observations. Here, the comparison is not as good as in the previous case. We even note a phase opposition between the two indices around 2000.7.

Table 2. Index Parameters

Index	$\langle s_i \rangle$	σ_i	R_i	R_i/σ_i
Lyα	5.350×10^{11}	0.318×10^{11}	0.236	0.743
F10.7	179.1	29.1	33.5	1.152
E10.7	177.3	25.6	25.6	1.001
MgII	0.2697	3.01×10^{-3}	2.23×10^{-3}	0.741

[21] The residual R_i between the predicted values f_i and the observed values s_i is equal to $\sqrt{< s_i > - < f_i >^2}$.

[22] As in the previous section, the solar Lyα flux index and solar MgII ratio index give the best results. The F10.7 and E10.7 results are mainly limited by the physical difference between the solar radio flux and the UV flux. For instance in Figure 3, there is an actual phase opposition around 2000.7 between the SWAN data and the F10.7 values. This is not the case in Figure 2. The peak value in F10.7 data around 2000.35 seen in Figure 3 is absent in Figure 2. The shortcomings of the F10.7 index in predicting EUV and UV fluxes variations have been documented by many authors [e.g. *Tobiska et al.*, 2000; *Woods et al.*, 2000]. Given the very restrictive assumption used by this algorithm, i.e. that solar activity on a scale smaller than 14 days can be neglected, we still get a very good forecast method for the solar Lyα flux and the solar MgII index and a fairly good forecast of the F10.7 (or the corrected E10.7) index. However, recent studies have shown that atmospheric drag is better correlated to the solar MgII index than to the F10.7 index (Thuillier, 2001, private communication). This stresses the potential relevance of our proposed sky Lyα method for a forecast of orbital decay.

4. Conclusion

[23] We have shown that it is possible to use outputs from the SWAN farside imaging technique to forecast the values of various solar indices half a solar rotation in advance.

[24] The accuracy of the forecasting technique depends on the actual correlation between the solar Lyα flux and the considered solar index. The MgII solar index is well correlated to the solar Lyα flux. This results in a good accuracy in the forecast. The result in the case of the 10.7 cm solar flux is less good. The accuracy is improved when using the E10.7 corrected index proposed by *Tobiska et al.* [2000].

[25] Direct comparison of the solar Lyα flux seen at Earth with the results of the SWAN flux maps indicate that the amplitude of the rotational modulations in the SWAN data is smaller than the amplitude of the illuminating solar flux. The derived damping of the amplitude is 13%. We suggest that this is a proof that multiple scattering effects cannot be neglected in this study.

[26] Future works will be developed to improve the retrieval of the SWAN flux index. As mentioned above, we need to include a better representation of the scattering process to achieve a better accuracy in the determination of the farside to nearside flux ratio.

[27] Another development will adapt our algorithm to retrieve all values between one day and a full solar rotation. This will allow us to give forecast values covering a full solar rotation in time, although the accuracy will decrease with longer time periods.

[28] SOHO is a mission of international cooperation between ESA and NASA. SWAN was financed in France by CNES with support from CNRS and in Finland by TEKES and the Finnish Meteorological Institute.

[29] **Acknowledgments.** The Editor would like to thank the reviewer of this manuscript.

References

Bertaux, J. L., E. Kyrölä, and E. Quémerais et al., SWAN: a study of Solar Wind Anisotropies on SOHO with sky mapping, *Solar Physics*, *162*, 403, 1995.

Bertaux, J.-L., E. Quémerais, R. Lallement, E. Lamassoure, W. Schmidt, and E. Kyrölä, Monitoring solar activity on the far side of the Sun from sky reflected Lyman alpha radiation, *Geophys. Res. Lett.*, *27*, 1331, 2000.

Fontenla, J., E. J. Reichmann, and E. Tandberg-Hanssen, The Lyman-alpha line in various solar features. I - Observations, *Astrophysical Journal*, *329*, 464, 1988.

Hall, D., Ultraviolet resonance radiation and the structure of the heliosphere, PhD Thesis, University of Arizona, 1992.

Quémerais, E., and J.-L. Bertaux, Radiative transfer in the interplanetary medium at Lyman alpha, *Astronomy and Astrophysics*, *277*, 283, 1993.

Quémerais, E., B. R. Sandel, and G. de Toma, 26 Day Modulation of the Sky Background LY alpha Brightness: Estimating the Interplanetary Hydrogen Density, *Astrophysical Journal*, *463*, 349, 1996.

Quémerais, E., Angle dependent partial frequency redistribution in the interplanetary medium at Lyman alpha, *Astronomy and Astrophysics*, *358*, 353, 2000.

Scherer, H., and H. J. Fahr, H Lyman alpha transport in the heliosphere based on on an expansion into scattering hierarchies, *Astronomy and Astrophysics*, *309*, 957, 1996.

Tobiska, W. K., T. Woods, F. Eparvier, R. Viereck, L. Floyd, D. Bouwer, G. Rottman, and O. R. White, The SOLAR2000 empirical solar irradiance model and forecast tool, *J. Atm. Terr. Phys.*, *62*(14), 1233, 2000.

Woods, T., W. K. Tobiska, G. J. Rottman, and J. R. Worden, Improved solar Lyman alpha irradiance modeling from 1947 through 1999 based on UARS observations, *J. Geophys. Res.*, *105*, 27,195–27,215, 2000.

Eric Quémerais and Jean-Loup Bertaux, Service d'Aéronomie du CNRS, B.P. 3, 91371, Verrières le Buisson, France. (eric.quemerais@aerov. jussieu. fr; jean-loup.bertaux@aerov.jussieu.fr)